Chemical Force Microscopy Study of Adhesive Properties of Polypropylene Films: Influence of Surface Polarity and Medium

Svetlana Gourianova, Norbert Willenbacher, and Michael Kutschera*

BASF Aktiengesellschaft, Polymer Physics, 67056 Ludwigshafen, Germany

The adhesive properties of untreated and corona treated polypropylene (PP) films were studied in polar (water) and nonpolar (hexadecane) liquid medium by using chemical force microscopy. A gold-coated colloidal probe was sequentially modified with self-assembled monolayers (SAMs) of ω-functionalized alkanethiols. The same colloidal probe was used for the force measurements, to avoid influence of determination accuracy of the spring constant and sphere radius on the obtained results. The thermodynamic work of adhesion was determined from the measured pull-off force using the Johnson−Kendall−Roberts (JKR) adhesion theory. Rabinovich's model was applied for the consideration of an effect of roughness when calculating the work of adhesion. It was found that the work of adhesion correlates with the hydrophilic properties of the PP surface and SAMs as well as with the polarity of the liquid medium. The observed correlations agree well with those found for the work of adhesion calculated from contact angle measurement.

1. Introduction

Control of the adhesion properties of polymer surfaces is crucial in many fields such as painting, printing, adhesive bonding, lamination to other films, and other coating applications.[1] The final product performance depends on the surface properties of the polymeric material. Commercially widely used polypropylene films have essentially hydrophobic surfaces, and their processing is nearly impossible without further surface modification like introduction of polar functional groups. Corona treatment is a common surface modification technique used for plastics and especially for polyolefins to generate these groups.[2]

Atomic force microscopy (AFM) has appeared to be an appropriate and reliable method for the investigation of adhesion phenomena. AFM combines very good lateral resolution and direct measurement of interaction between AFM probe and sample. Most of the studies of adhesion properties by AFM described in the literature relate to model systems such as interaction between two self-assembled monolayers (SAM−SAM)[3−6] but rarely to technically relevant systems, which are considerably more complex; for example, for polymer surfaces, numerous factors such as roughness, morphology, and viscoelastic phenomena hinder the correct interpretation of adhesion measurements.

This work aims to use the colloidal probe technique for a correlation of adhesion properties with molecular characteristics of polymer surfaces. In this article, the adhesive properties of untreated and corona treated polypropylene film surfaces versus various chemical groups deposited onto an AFM colloidal probe and the dependence of adhesion forces on the polarity of the surrounding liquid medium are presented.
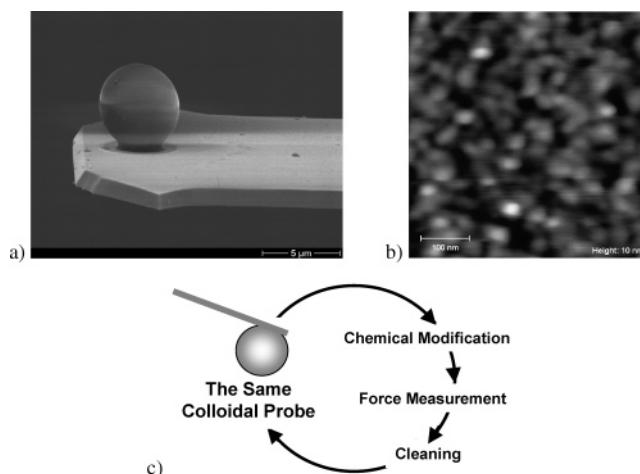

Figure 1. (a) SEM image of a gold-coated silica sphere on the end of a rectangle cantilever, (b) contact mode AFM height image of a gold-coated silica sphere, and (c) schematic view of the colloidal probe preparation procedure.

2. Experimental Section

Materials. *Polypropylene Film.* The film used in this study was commercial 35 μm thick, heat sealable, coextruded biaxially oriented polypropylene (BOPP) film Bicor MB400 (Exxon Mobil Chemical). The commercial BOPP films are usually corona treated on one side immediately after manufacturing. For our investigation, we used the untreated side of the film. Before usage, the PP film was rinsed with water and dried for 1 h in a vacuum at room temperature.

Alkanethiols. Octadecylmercaptan ($CH_3(CH_2)_{17}SH$, 98%, Aldrich), 11-mercapto-1-undecanol ($OH(CH_2)_{11}SH$, 97%, Aldrich), 16-mercaptohexadecanoic acid ($COOH(CH_2)_{15}SH$, 90%, Aldrich), and 11-amino-1-undecanethiol ($NH_2(CH_2)_{11}SH$, >90%, Dojindo Laboratories) were used as received.

Liquids. The water used in this study was Millipore water (18 MΩ·cm) purified by a Millipore water purification system (Millipore GmbH, Eschborn, Germany). Ethanol (Uvasol, ≥99.9%, Merck KGaA), hexadecane (>99%, Merck), diiodomethane (99%, Aldrich), and formamide (≥99.5%, Fluka) were used as received.

Preparation and Chemical Modification of the Colloidal Probe. A micron-sized silica sphere (Bangs Laboratories, Inc., SS06N/4907) of 6.1 μm diameter was attached to the free end of a tipless silicon cantilever (MikroMasch, CSC12, no coating,

* To whom correspondence should be addressed. E-mail: michael.kutschera@basf-ag.de.

(1) Brewis, D. M. *Prog. Rubber Plastic Technol.* **1985**, *1*, 1.
(2) Kinloch, A. J. *Adhesion and Adhesives, Science and Technology*; Chapman and Hall: London, 1990.
(3) Papastavrou, G.; Akari, S. *Colloids Surf., A* **2000**, *164*, 175−181.
(4) Noel, O.; Brogly, M.; Castelein, G.; Schultz, J. *Langmuir* **2004**, *20*, 2707−2712.
(5) Clear, S. C.; Nealey, P. F. *J. Colloid Interface Sci.* **1999**, *213*, 238−250.
(6) Frisbee, C. D.; Rozsnyai, L. F.; Noy, A.; Wrighton, M. S.; Lieber, C. M. *Science* **1994**, *265*, 2071−2074.
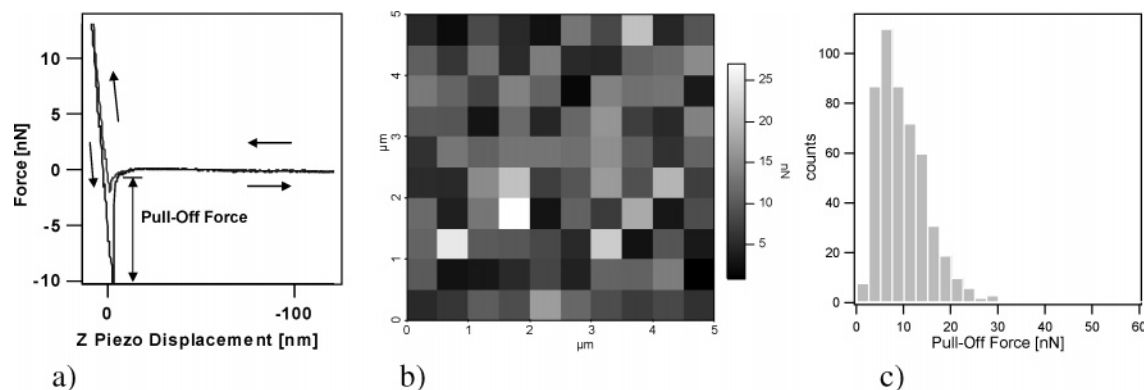
Figure 2. (a) Typical force vs Z piezo displacement curve, (b) force volume image, and (c) histogram of adhesion forces between corona treated polypropylene film and colloidal probe modified with $-NH_2$ functionality measured in water.

length 90 μm, nominal spring constant (k) 1.75 N/m, actual spring constant measured by the thermal oscillation method[7] 2.1 N/m) with Norland Optical UV-adhesives NOA63 using a three-dimensional microtranslation stage (Micro Controle) and optical microscope system. The adhesives were subsequently cured by exposure to UV light.

The colloidal probe was coated with 5 nm of chromium as the adhesion promoting layer, followed by 50 nm of gold by means of thermal evaporation (evaporation rate 2 Å/s, pressure 4 × 10^{-5} mbar). The cantilever with attached silica sphere was coated on both sides to avoid bending due to the different thermal expansion coefficients of metal and silicon. Figure 1a and b shows a scanning electron microscopy (SEM) image of the colloidal probe and a contact mode AFM height image (500 nm × 500 nm) of a surface of a gold-coated silica sphere. The root-mean-square (rms) surface roughness of the surface is 1.2 nm calculated over an area of 1 μm^2.

Before the SAM preparation, the gold-coated colloidal probe was cleaned in oxygen plasma (15 min, 7 × 10^{-2} mbar, 50 W RF power), which was followed by immersion into pure hot ethanol at ~70 °C for 15 min to reduce surface gold oxide.[8–10] The freshly cleaned colloidal probe was then immersed into 1 mM ethanolic solutions of various alkanethiols at room temperature for 24 h. Upon removal, the probe was rinsed thoroughly with absolute ethanol. To ensure that no ethanol remained on the surface, the probe was placed in an oven at 80 °C for 20 min. After this preparation, the colloidal probe was immediately used for the adhesion measurements. First, the measurements were carried out on all samples in water; after that, the colloid probe was dried and used for the next measurements in hexadecane.

For the purpose of comparability of the results obtained, *the same colloidal probe* was subsequently coated with various SAMs (Figure 1c), to avoid the influence of differences in surface roughness of the silica spheres as well as the influence of determination accuracy of parameters such as sphere radius and spring constant on the measured adhesion forces. After each adhesion measurement, the colloidal probe was cleaned again as described above. The 15 min of 50 W O$_2$ plasma treatment are sufficient to completely remove the SAM from the gold surface.[11] This was also verified in the present work. The flat substrates cut from a silicon wafer were prepared in the same way as the colloidal probe and used for quality control of surface modification by X-ray photoelectron spectroscopy and contact angle measurements.

Corona Treatment of PP Film. Corona treatment was carried out on a corona station manufactured by Softal Electronic GmbH, type 6020. The gap between the electrode and the sample is 2 mm. The films were exposed to one pass in ambient air at a speed of 50 m/min. The energy delivered to the surface during treatment was 4 kJ/m^2. The low molecular weight oxidized material generated by corona treatment was removed from the

film surface by water rinsing, to avoid dissolving of this material during the force measurement in liquid medium.

Contact Angle Measurement and Analysis. The contact angles of water, formamide, and diiodomethane on PP films and SAMs were measured by a video based contact angle analyzer (Krüss, model DSA 10-Mk2), to evaluate the surface energy of the samples and to ensure the formation of high quality SAMs.

The polar (γ_s^p) and nonpolar (γ_s^d) components and the total surface energy (γ_s) were evaluated by application of the Owens and Wendt equation:[12]

$$(1 + \cos\theta)\gamma_l = 2[(\gamma_s^d + \gamma_l^d)^{1/2} + (\gamma_s^p + \gamma_l^p)^{1/2}] \qquad (1)$$

$$\gamma_s = \gamma_s^d + \gamma_s^p \qquad (2)$$

where θ, γ_l, and γ_l^d and γ_l^p denote the contact angle, the surface tension of liquids, and the nonpolar and polar components of the surface tension of the liquids, respectively.

The contact angles of hexadecane and water on the studied samples were measured in order to evaluate the interface energy between "solid" surfaces and liquid medium, in which force measurements were carried out, using Young's equation as described in detail below.

X-ray Photoelectron Spectroscopy (XPS). The surface chemical analysis of SAMs and PP films was confirmed using an XPS/ESCA Phi 5600LS spectrometer (Physical Electronics) with an Al Kα source, which was operated at 300 W. Survey and high resolution spectra were obtained at a takeoff angle of 45° using a beam size of 800 μm and pass energies of 11.75 and 117.4 eV, respectively. A charge neutralization system with a low energy electron flood neutralizer and a low energy ion beam neutralizer was used to compensate a sample charging.

Surface Imaging. Surface imaging was carried out with a Nanoscope III Multimode atomic force microscope (Digital Instruments, Santa Barbara) in air in contact mode with a Si cantilever (spring constant 1.4–4.1 N/m, length 224 μm, Nanosensors) and in tapping mode with a Si cantilever (spring constant 42 N/m, length 160 μm, Olympus). For analysis of the surface roughness, the rms value was used.

Adhesion Force Mapping. The force measurements were performed on a molecular force probe 3D (MFP-3D) atomic force microscope (Asylum Research, Santa Barbara) in a liquid medium (water and hexadecane) at room temperature. The instrumentation and approach to force measurement using the MFP-3D atomic force microscope was described in details by Hammond et al.[13]

The adhesive interaction between colloidal probe and sample was determined from force versus Z piezo displacement curves. An example is shown in Figure 2a. The cantilever deflection was recorded as the sphere approaches, contacts, and then withdraws from the sample. The observed cantilever deflection was converted

(7) Hutter, J. L.; Bechhoefer, J. *Rev. Sci. Instrum.* **1993**, *64*, 1868.
(8) Sato, F.; Okui, H.; Akiba, U.; Suga, K.; Fujihira, M. *Ultramicroscopy* **2003**, *97*, 303–314.
(9) Ron, H.; Rubinstein, I. *Langmuir* **1994**, *10*, 4566–4573.
(10) Tsai, M. Y.; Lin, J. C. *J. Colloid Interface Sci.* **2001**, *238*, 259–266.
(11) Elms, F. M.; George, G. A. *Polym. Adv. Technol.* **1998**, *9*, 31–37.

(12) Owens, D. K.; Wendt, R. C. *J. Appl. Polym. Sci.* **1969**, *13*, 1741–1747.
(13) Jiang, X.; Ortiz, C.; Hammond, P. T. *Langmuir* **2002**, *18*, 1131–1143.
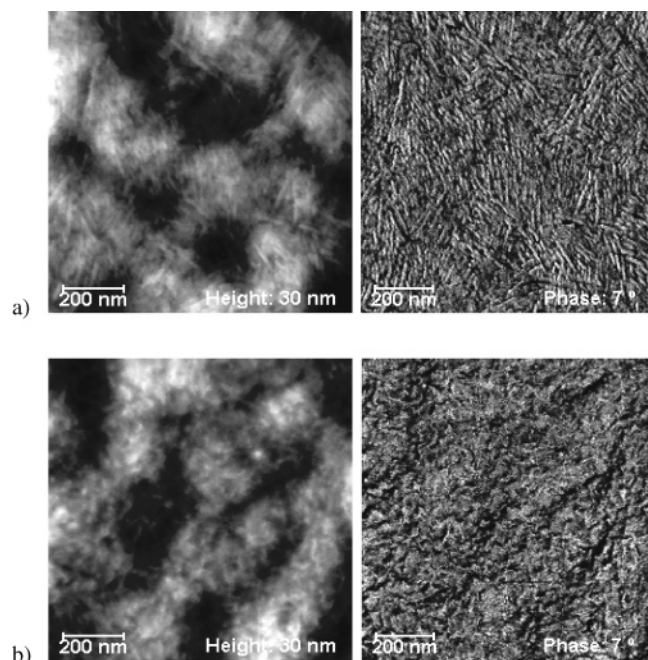
Figure 3. Tapping mode AFM height and phase image of water-rinsed polypropylene films (a) before (rms = 5.5 nm) and (b) after (rms = 5.2 nm) corona treatment.

into force using the spring constant of the cantilever. The motion of the sphere was changed from approach to retract when the cantilever deflection was equal to a trigger value of 10 nm. Therefore, the force introduced by the cantilever was kept to a constant low level of approximately 21 nN. The additional intrinsic adhesion forces between sphere and sample depend on the specific surfaces and are the subject of our investigation. All measurements were performed with a frequency of approach/retract cycle of 1 Hz, with a ramp size of 640 nm, and captured with a resolution of 5000 points per curve.

The surface of PP film has a relative high roughness (rms = 5.5 nm) and is not absolutely homogeneous because of the presence of additives. Therefore, force versus displacement curves were collected using "force volume" mode over surface area $5 \mu m \times 5 \mu m$ at a resolution of 10×10 pixels (100 force curves) for collecting statistics and averaging surface properties. The radius of contact area at separation (a_s) determined from pull-off force by applying the Johnson–Kendall–Roberts (JKR) contact theory is about 10–100 nm. Thus, a theoretical lateral resolution of the method is higher than the resolution used in this study only for averaging surface properties. The force volume images (Figure 2b) were measured on three to five different places of the sample, resulting in 300–500 force versus distance curves collected for each SAM–PP film. The pull-off forces observed in individual approach/retract cycles were plotted in a histogram (Figure 2c), and mean value and standard deviation were determined for the adhesion interaction characterization.

3. Results and Discussion

Surface Characterization of PP Films. The surface morphology of the PP film (Figure 3a) shows a fibrillar structure with biaxial orientation of the crystalline lamellae typical for BOPP, as already described in the literature.[14,15] For a characterization of physicochemical surface properties of untreated (PP) and corona treated (PPcorona) polypropylene film, we used two methods: contact angle measurement and X-ray photoelectron spectroscopy. From contact angles of several polar and nonpolar liquids on polypropylene films, the surface energy (γ) and its polar (γ^p) and dispersive (γ^d) components

Table 1. Measured Contact Angles and Calculated Surface Energies for Polypropylene Films, a Gold Surface, and Various SAMs

	contact angle (θ, deg)			surface energy (mN/m)		
	water	diiodo-methane	formamide	γ^d	γ^p	γ_{total}
substrate						
PP	111.0	69.2	93.3	21.5	0.0	21.5
PPcorona	61.7	35.6	54.7	35.3	11.2	46.5
probe						
Au[a]	60.8	25.7	46.0	45.9	0.1	46.0
$-CH_3$	107.2	72.4	88.7	20.6	0.3	20.9
$-NH_2$	50.1	28.7	41.3	38.5	16.3	54.8
$-OH$	16.9	26.8	8.5	38.9	31.6	70.5
$-COOH$	12.6	33.5	6.8	36.7	34.2	70.9

[a] After cleaning in oxygen plasma with subsequent washing in hot ethanol.

were calculated using Owens and Wendt theory (Table 1). From Table 1, it can be seen that the untreated PP film is very hydrophobic (contact angle for water 111°) and the surface energy of the film is mainly controlled by the dispersive component. The reason is the chemical structure of PP, which does not have any polar functional groups, as was confirmed by surface chemical analysis with XPS. The XPS spectra (Figure 4) and the surface atomic percentage (Table 2) show that almost only carbon was detected on the surface of the untreated PP; hence, the surface can be considered as "clean".

Figure 3b shows the corona treated film after water rinsing. It can be seen that the corona treatment caused evident changes in the surface morphology. The fibrillar structure was destroyed because of oxidation and chain scission processes during corona treatment. The removal of the thereby generated low molecular weight oxidized material by water rinsing does not turn the surface structure into the original one. This observation agrees well with the work of Strobel et al.[16] and O'Hare et al.[15] The XPS analysis (Figure 4, Table 2) shows that the oxygen content is much higher compared to the untreated film surface. On the basis of the C1s spectra, it can be concluded that corona treatment incorporated 4 atom % of hydroxyl (C–OH) and peroxy (C–O–O) functional groups with a binding energy shift of 1.4 eV relative to hydrocarbon at 284.8 eV. The presence of these groups makes the surface more hydrophilic and leads to a decrease of the contact angle of water and to an increase of the film surface energy from 21.5 to 46.5 mN/m (Table 1).

Despite some changes in morphology, the use of a corona energy of 4 kJ/m² leads only to a slightly decrease of rms surface roughness, which influences the sphere–sample contact area, from 5.5 nm (over an area of 1 μm²) for untreated PP film to 5.2 nm for corona treated film. The sphere–sample contact area depends not only on surface roughness but also on mechanical properties of the films. To compare these, we present in Figure 5 the extension part of force versus separation curves measured on both treated and untreated PP films and on silicon wafer. The curves were obtained from the corresponding force versus displacement curves by accounting for the cantilever deflection on a rigid surface[17] (silicon wafer). From Figure 5, it can be seen that at the low maximum load force we used combined with the comparatively big colloidal probe the surfaces of polymer films are not deformed or at least

(14) Boyd, R. D.; Kenwright, A. M.; Badyal, J. P. S. *Macromolecules* **1997**, *30*, 5429.

(15) O'Hare, L. A.; Leadley, S.; Parbhoo, B. *Surf. Interface Anal.* **2002**, *33*, 335–342.

(16) Strobel, M.; Dunatov, C.; Strobel, J. M.; Lyons, C. S.; Perron, S. J.; Morgen, M. C. *J. Adhes. Sci. Technol.* **1989**, *3*, 321.

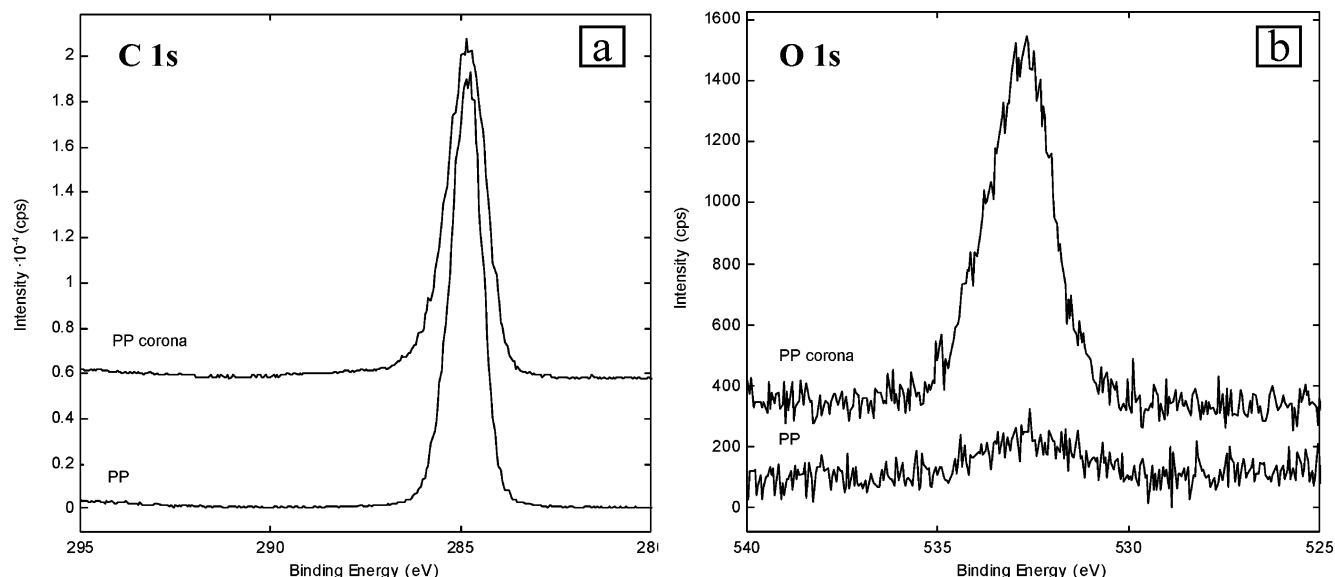(17) Kappl, M.; Butt, H.-J. *Part. Part. Syst. Charact.* **2002**, *19*, 129–143.

Figure 4. XPS C1s (a) and O1s (b) spectra of water-washed polypropylene films before (PP) and after corona treatment with subsequent water washing (PP corona).
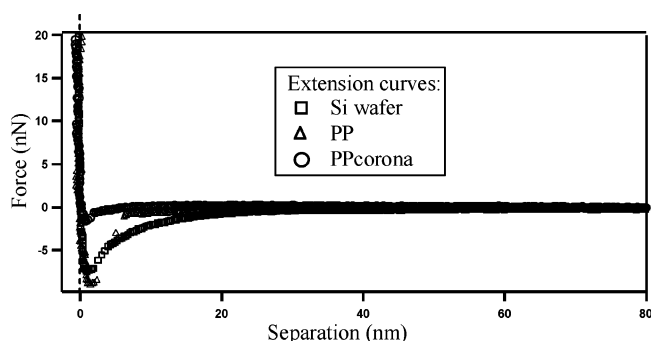

Figure 5. Extension part of force vs separation curves measured with a colloidal probe coated by NH_2−SAM on both untreated and corona treated PP films and silicon wafer in water.

Table 2. Surface Atomic Percentage of Untreated (PP) and Corona Treated (PPcorona) Polypropylene Films

	C (atom %)	O (atom %)
PP	99.7	0.3
PPcorona	97.9	2.1

deformation is below the experimental resolution and negligible. This means that there should be no significant difference in contact area between the sphere and both PP films and a direct comparison of the measurement results on both surfaces is possible.

Characterization of SAMs. For physicochemical characterization of SAMs, gold-coated Si wafers were used as substrates. The contact angle values and surface energies evaluated by the application of the contact angle data to eq 1 are shown in Table 1 for the Au layer and for the SAMs terminated with various functional groups. A clean gold surface should be very hydrophilic.[18] However, the contact angle of water on gold increases to 60° in a few minutes of gold exposure to a laboratory environment (Table 1). This is attributed to the formation of carbonaceous contamination on the gold surface. The XPS results (Table 3) show that C, O, and even small traces of N and S were detected on the Au surface. The source of this contamination is the laboratory environment. The very small sulfur peak in the Au-cleaned sample was observed

at around 168 eV attributed to the sulfoxide species. Tarlov et al.[19] and Ishida et al.[20] claim that sulfoxide species can be removed in ethanolic thiol solution easily during the immersion time used in this work and do not compete with thiol molecules. In our experiments, we even went further and cleaned the surfaces in hot ethanol immediately before thiol modification and immersed them in ethanolic thiol solution without drying. Therefore, the samples are not at all exposed to the laboratory environment between cleaning and thiol surface modification. On the other hand, all samples analyzed by XPS have been exposed to laboratory air (sample transfer) for some time and are therefore contaminated.

As shown in Table 1, the value of the total surface energy of hydrophobic CH_3-thiol is low, composed mainly of a nonpolar dispersive component and very similar to the untreated PP surface. The surface energy values of hydrophilic OH- and COOH-thiols are high, and the polar component is about 50% of the total surface energy. The observed contact angle and surface energy values correspond well with previous reports[21−23] for Au and OH-, COOH-, and CH_3-thiol SAMs. The observed contact angle of water on a SAM of NH_2-thiol is higher than that observed by Tanahashi et al.[23] but is in good agreement with the results obtained for NH_2-silane SAMs.[4,24] We attribute this to a more perfect SAM formation in this work. The hydrophobic properties of SAMs were found in the order CH_3 > NH_2 > OH > COOH. This correlation of hydrophobic−hydrophilic character of the end group of the SAMs and contact angle measurements confirms the successful formation of SAMs on the gold surface.

The procedure of chemical modification of the colloidal probe used in this work differs from the usual preparation of SAMs known in the literature. We used *the same colloidal probe* for the sequential coating with various SAMs. This involves an additional step: removal of the

(18) Smith, T. *J. Colloid Interface Sci.* **1980**, *75*, 51−55.

(19) Tarlov, M. J.; Burgess, D. R. F.; Gillen, G. *J. Am. Chem. Soc.* **1993**, *115*, 5305.

(20) Ishida, T.; Tsuneda, S.; Nishida, N.; Hara, M.; Sasabe, H.; Knoll, W. *Langmuir* **1997**, *13*, 4638−4643.

(21) Lin, J. C.; Chuang, W. H. *J. Biomed. Mater. Res.* **2000**, *51*, 413−423.

(22) Ahn, H. S.; Cuong, P. D.; Park, S.; Kim, Y. W.; Lim, J. C. *Wear* **2003**, *255*, 819−825.

(23) Tanahashi, M.; Matsuda, T. *J. Biomed. Mater. Res.* **1997**, *34*, 305−315.

(24) Tsukruk, V. V.; Bliznyuk, V. N. *Langmuir* **1998**, *14*, 446−455.

Table 3. Surface Atomic Percentage of Au Substrates and SAMs Terminated with Various Functional Groups

	C (atom %)	O (atom %)	N (atom %)	S (atom %)	Au (atom %)
cleaning of Au surface					
Au[a]	27.3	4.6	0.3	0.3	67.4
Au cleaned[b]	26.3	3.4	0.8	0.3	69.2
SAM surface					
SH(CH$_2$)$_{15}$COOH	54.9	7.5		2.2	35.3
SH(CH$_2$)$_{11}$NH$_2$	49.5	2.4	3.4	2.1	42.5
SH(CH$_2$)$_{11}$OH	54.5	4.4		2.0	39.1
SH(CH$_2$)$_{17}$CH$_3$	58.0	0.4		1.9	39.7

[a] Fresh evaporated gold surface after cleaning in oxygen plasma with subsequent washing in hot ethanol. [b] The modified with NH$_2$-thiol SAM gold surface after cleaning in oxygen plasma with subsequent washing in the hot ethanol.

old SAM. To show that the cleaning procedure used in this work is able to remove the SAM from the gold surface, XPS measurements were carried out on a sample ("Au cleaned", Table 3), which was at first modified with a NH$_2$-thiol SAM and after that cleaned in oxygen plasma with subsequent washing in the hot ethanol, as described in the Experimental Section. The comparison of the elemental composition of this sample with the results obtained on the Au layer without prior coating with a SAM confirms the effective removing of thiol coating. This was also checked for all other SAM types used.

To ensure the formation of the new SAMs on the cleaned gold surface by XPS, the modification of the same substrate was carried out in the follow order: COOH → NH$_2$ → OH → CH$_3$. Upon treatment with thiols, the atomic percentage of Au significantly decreased, whereas the atomic percentage of C and S increased. For the COOH-thiol, a higher content of O was found. For the alkanethiol with the −NH$_2$ end group, nitrogen atoms were newly detected, which were later completely removed before the next modification with OH-thiol. The surface composition of gold surface modified with CH$_3$-thiol consists mainly of C, S, and Au. For all surfaces studied, the S atomic concentration was lower than the expected value. This is due to the fact that the thiols are highly oriented on the surface and the signal information from the gold−thiol interface is attenuated by the (CH$_2$)$_X$ spacer.

The XPS results confirm the efficiency of the surface cleaning procedure and indicate that the alkanethiols were firmly deposited on the gold surface.

The study of the SAM surface morphology was made by AFM. Figure 6a shows the height and phase contrast images of a gold surface after cleaning with O$_2$ plasma with subsequent ethanol washing. Figure 6b shows the images of the gold surface coated with a SAM of COOH-thiol, which is representative of all SAMs used. The roughness of the thiol-coated surface of 0.8 nm over an area of 1μm^2 is the same as that observed on the pure gold surface. The phase contrast image shows the surface to be homogeneous. These observations confirm that no aggregates were formed and there is a complete homogeneous coverage of the surface.

Determination of Thermodynamic Work of Adhesion from Pull-Off Force Measurement via JKR Adhesion Model. The force versus displacement curves were collected in the force volume mode described in the Experimental Section. This mode allows a statistic averaging of the surface properties. This has two distinct advantages. First, the effects of the surface roughness of the PP film and therefore changing contact area are averaged. Second, surface inhomogeneities due to additives or contamination can be identified and excluded from the results. Figures 7 and 8 show the representative force versus displacement curves for all studied SAM−polypropylene film combinations measured in water and hexadecane, respectively. From the collected curves, the pull-
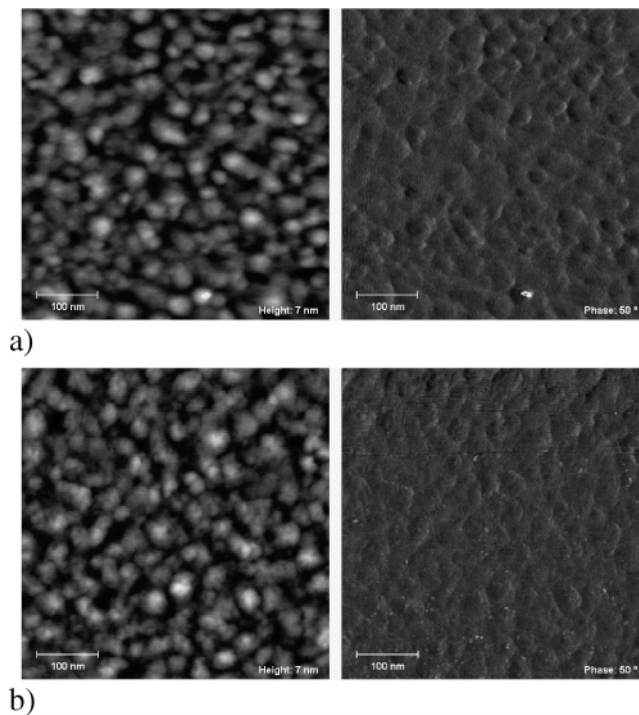

a)

b)

Figure 6. Tapping mode AFM height (left) and phase (right) images of (a) a gold-coated Si wafer surface after the cleaning procedure (rms = 0.8 nm) and (b) a gold surface with a SAM of 16-mercaptohexadecanoic acid (rms = 0.8 nm).

off forces and their average values were extracted for each SAM−polymer film combination.

In a force versus piezo displacement curve, the attractive forces are negative. In Figure 9, the absolute values of normalized pull-off forces ($F_{pull-off}/R$) and their standard deviation are shown. The high standard deviations (up to 50% of the force value) are partially attributed to the inherent fluctuations of pull-off forces,[25] partially to the variation of the contact areas between probe and sample because of roughness[26] and to inhomogeneities on the film surface, as mentioned above.

The obtained results show that the adhesion forces are sensitive to the chemical composition of the polypropylene film surface, to the functionality on the colloidal probe, and to the surrounding liquid medium, in which the measurements were carried out. It can be seen (Figure 9a) that in water the pull-off force values measured on hydrophobic untreated PP are higher than those on corona treated film, whereas the adhesion forces on both samples decrease linearly if the hydrophilicity of the SAMs on the

(25) (a) Frisbie, D.; Rozsnyai, L. F.; Noy, A.; Wrighton, M. S.; Lieber, C. M. *Science* **1994**, *265*, 2071. (b) Noy, A.; Frisbie, D.; Rozsnyai, L. F.; Wrighton, M. S.; Lieber, C. M. *J. Am. Chem Soc*. **1995**, *117*, 7943.
(26) (a) Schönherr, H.; Vansco, G. *J. ACS Polym. Div. Polym. Prepr.* **1996**, *37*, 612. (b) Schönherr, H.; Vansco, G. *J Polym. Sci., Part B: Polym. Phys.* **1998**, *36*, 2483.
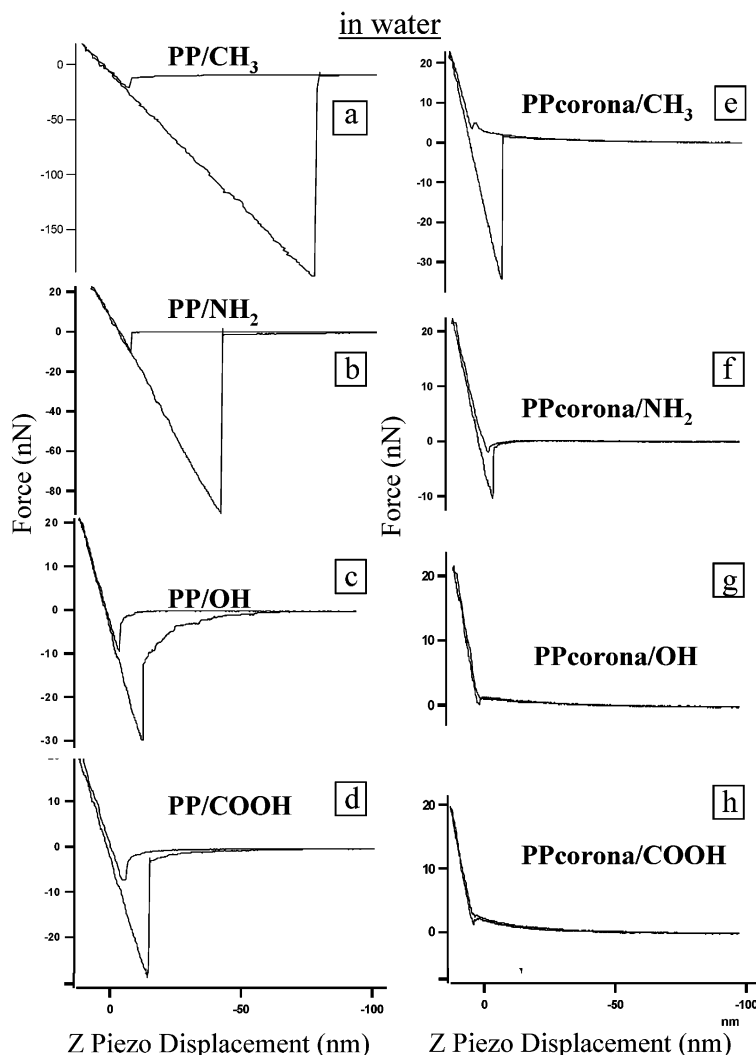
Figure 7. Representative force vs displacement curves for all studied surface compositions measured in water.

colloidal probe increases (the surface energy increases). In hexadecane (Figure 9b), a reverse situation can be observed. The pull-off force increases linearly with surface energy, and the adhesion to the corona treated film is higher than that to the untreated one.

The mechanical detachment force (pull-off force) can be related to the thermodynamic work of adhesion by applying one of the contact mechanics models. The Derjaguin−Müller−Toporov (DMT) model[27] is typically applied to tips with a high stiffness and a small curvature radius, that is, small contact radii. For the system studied in this work, we chose the JKR model.[28−30] JKR theory is applicable for the systems with large particle radii, high surface energies, and compliant materials under two main assumptions: the surfaces are elastic and smooth. The validity of the first assumption can be checked from the profile of the contact region in the force versus piezo displacement curve. For an ideal elastic sample surface, the loading and unloading curves overlap, while materials exhibiting plastic deformation or viscous creep show a hysteresis between the two curves.[31] In force versus

displacement curves (Figures 7 and 8), the contact lines are straight and little hysteresis is observed. Thus, the assumption of elasticity of PP films is valid for our case. The second assumption about perfectly smooth surfaces cannot be realized in a real experimental system. To consider the effect of surface roughness on the adhesion, a model proposed by Rabinovich et al.[32] was used, the details of which are described below. The thermodynamic work of adhesion (W_a) according to the JKR model is

$$W_a = -\frac{2}{3\pi}\frac{F_{\text{pull-off}}}{R} \tag{3}$$

The calculated values of W_a and their standard deviation are shown in Figure 10. One can see clearly that the interaction of two hydrophobic surfaces (PP/−CH$_3$) is strong in polar solvent (water) and very weak in nonpolar solvent (hexadecane), whereas the adhesion between two hydrophilic surfaces (PPcorona/−OH or PPcorona/−COOH) is stronger in hexadecane than in water. This indicates that adhesion depends strongly on the solvent free energy.

It is also known[33] that the −COOH groups of a SAM are deprotonated by pHs higher than 5.7. We measured[34] that not only the surface of corona treated PPcorona but also

(27) Derjaguin, B. V.; Muller, V. M.; Toporov, Y. P. *J. Colloid Interface Sci.* **1975**, *53*, 314.
(28) Johnson, K. L.; Kendall, K.; Roberts, A. D. *Proc. R. Soc. London, Ser. A* **1971**, *324*, 301.
(29) Kokkoli, E.; Zukoski, C. F. *J. Colloid Interface Sci.* **1999**, *209*, 60−65.
(30) Biggs, S.; Spinks, G. *J. Adhes. Sci. Technol.* **1998**, *12*, 461−478.
(31) Doerner, M. F.; Nix, W. D. *J. Mater. Res.* **1986**, *1*, 601−609.

(32) Rabinovich, Y. I.; Adler, J. J.; Ata, A.; Singh, R. K.; Moudgil, B. M. *J Colloid Interface Sci.* **2000**, *232*, 10−16.
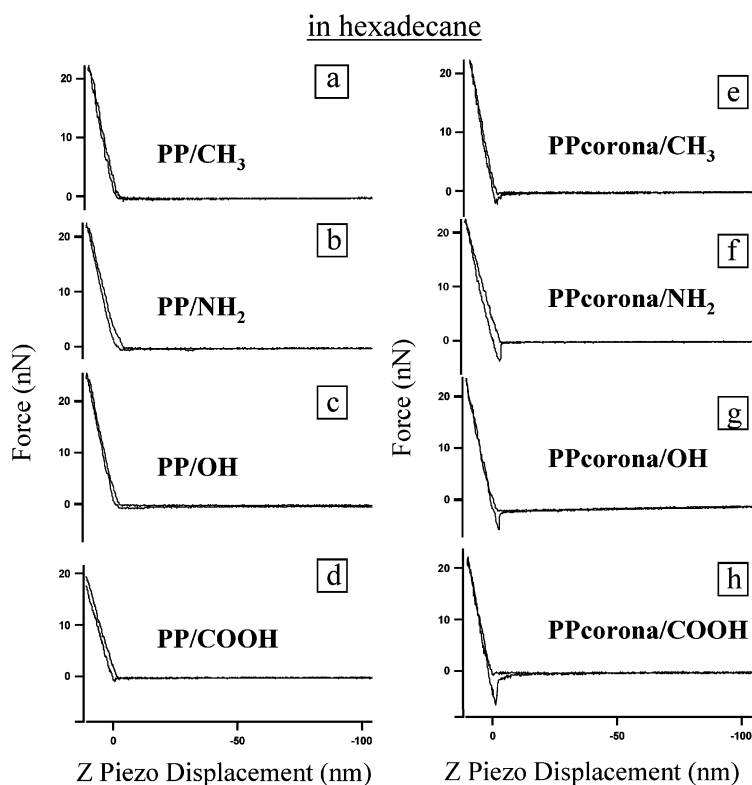
Figure 8. Representative force vs displacement curves for all studied surface compositions measured in hexadecane.
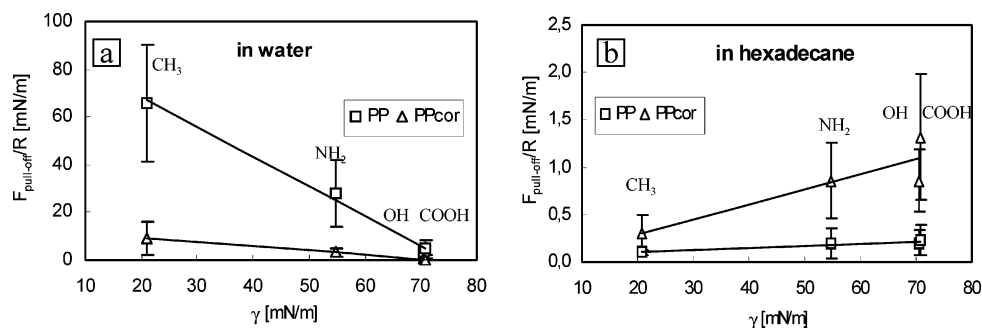

Figure 9. Normalized pull-off forces ($F_{\text{pull-off}}/R$) (R represents the radius of the colloidal probe) measured on PP and PPcorona (a) in water and (b) in hexadecane as a function of the total surface energy of SAMs on the colloidal probe.
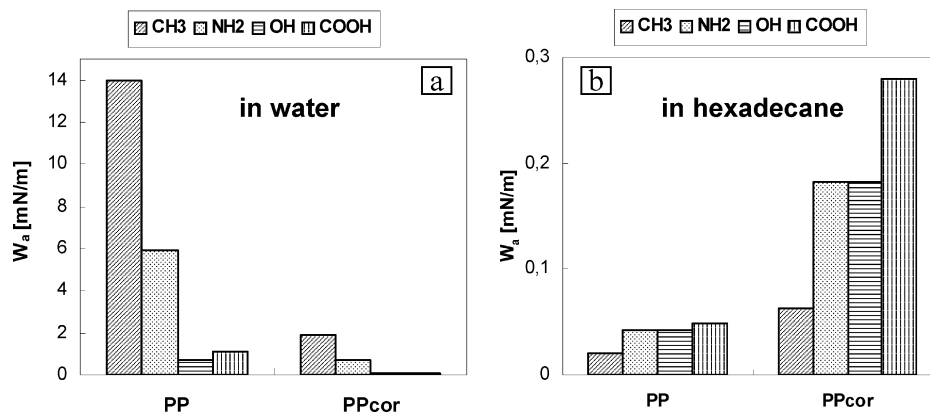

Figure 10. Work of adhesion determined from the results of AFM adhesion force measurement (a) in water and (b) in hexadecane, by applying the JKR adhesion model.

the surface of untreated PP is negative charged by pHs of 3.5 and higher. Hence, the long-range repulsive forces can be expected for the interaction of polypropylene films and −COOH in water by neutral pH used in this study. However, it can be seen from force versus displacement curves (Figure 7a−d) that only attractive forces act in water between the untreated PP sample and all studied functional groups. Obviously, attractive hydrophobic forces are much stronger than repulsive electrostatic forces. However, in the case of interaction between corona treated

Table 4. Measured Contact Angle (θ) and Calculated Interface Energy (γ)

X	contact angle (θ, deg)		interface energy ($\gamma_{X/Y}$, mN/m)			
	water	hexadecane	X/water	X/hexadecane	X/PP	X/PPcorona
substrate						
PP	111.0	<2	47.6	−5.9		
PP corona	61.7	<2	11.9	19.0		
SAM−surface						
−CH$_3$	107.2	36.4	42.4	−1.2	0.3	9.8
−NH$_2$	50.1	<2	8.1	27.3	18.8	0.6
−OH	16.9	5.5	0.8	43.1	34.2	5.3
−COOH	12.6	9.1	−0.2	43.8	36.2	6.3

film PPcorona and COOH−SAM in water (Figure 7h), the expected electrostatic repulsive forces can be observed, because, first, the hydrophobic forces are weaker and, second, the negative charge of the PPcorona sample is stronger than that of the PP sample.[33]

The adhesion of the untreated PP sample to hydrophilic OH− and COOH−SAMs as well as of the corona treated PPcorona sample to CH$_3$−SAM in water is higher compared to the adhesion for the same combinations in hexadecane. This can be explained by hydrophobic interaction too, because the presence of only one hydrophobic surface in water leads to a domination of hydrophobic forces over other interaction forces.[3]

In hexadecane (Figure 10b), the contribution of hydrophobic interaction disappears and the untreated PP has a very small adhesion to all SAMs used in this study. The low adhesion values in hexadecane are reasonable for the interaction between uncharged polar and nonpolar groups. For the combination PP/CH$_3$−SAM, no detectable adhesive jumps in the force versus distance curve were observed, due to the limit of the force resolution of the cantilever used. In this case, the value of noise on force versus distance curve was taken as the pull-off force value.

The XPS analysis shows that the corona treated PPcorona sample has C−OH and C−O−O groups on the surface, but it is likely that there are some other oxygen-containing groups such as COOH and C=O on the surface in very small concentration, as was observed in the literature.[15] These groups are able to build hydrogen bonds with OH−, NH$_2$−, and COOH−SAMs. Since hexadecane has a very low dielectric constant, one could conclude that the observed attractive forces are primarily due to electrostatic interactions based on the dipole moment of these groups, resulting in hydrogen bonds.[3]

In general, adhesion forces vary linearly with surface energy for the systems investigated here (see Figure 9). For the systems PPcorona/COOH−SAM and PPcorona/OH−SAM in hexadecane, the pull-off forces are equal within experimental uncertainty, but there seems to be a trend that the adhesion force to COOH−SAM is higher than that to OH−SAM. The reasons for this could be, first, the stronger hydrogen bonding for −COOH/−OH and −COOH/−COOH pairs than for −OH/−OH pairs, second, in nonpolar solvent, the −COOH/−COOH groups can build two hydrogen bonds per single pair of groups (dimer formation), and, third, other interactions, for example, chemical bonding between −COOH and −OH groups, can be supposed.

Determination of Thermodynamic Work of Adhesion from Contact Angle Measurements. To verify the results obtained by AFM, contact angle measurements were used for calculating the thermodynamic work of adhesion. The work of adhesion per unit contact area is related to interface energy values by the Dupre equation: [35]

$$W_a = \gamma_{13} + \gamma_{23} - \gamma_{12} \qquad (4)$$

where γ_{13} is the solid 1 (sample)/medium interface energy, γ_{23} is the solid 2 (colloidal probe)/medium interface energy, and γ_{12} is the solid 1/solid 2 (sample/colloidal probe) interface energy. The sample/colloidal probe interface energies were estimated from the Fowkes equation using surface energies and their polar and nonpolar components (Table 1):

$$\gamma_{12} = \gamma_1 + \gamma_2 - 2[(\gamma_1^d + \gamma_2^d)^{1/2} + (\gamma_1^p + \gamma_2^p)^{1/2}] \quad (5)$$

The solid/liquid medium interface energies were estimated using surface energies of solids from Table 1 and of liquids (72.8 mN/m for water and 27.5 mN/m for hexadecane) and contact angles for liquids from Table 4 using the Young equation:

$$\gamma_{13} = \gamma_1 - \gamma_3 \cos \theta_1 \qquad (6)$$

$$\gamma_{23} = \gamma_2 - \gamma_3 \cos \theta_2 \qquad (7)$$

The results of contact angle measurements and of calculations of interface energies are displayed in Table 4.

Figure 11 shows the work of adhesion for all studied surface combinations derived from contact angle measurement. At this place, it should be noted that the Young equation is valid for finite contact angles in the case of mechanical equilibrium and does not apply when spreading takes place.[36] The contact angles for hexadecane on all studied surfaces, except CH$_3$−SAM, are smaller than 10° (Table 4). This means that the values of the surface energy and thus of the work of adhesion obtained by using these contact angles must be interpreted and used carefully.

The derived work of adhesion for interaction between hydrophobic PP/CH$_3$−SAM surfaces in water (89.7 mN/m, Figure 11a) agrees well with the literature values (92−103 mN/m) obtained for interaction in the chemically similar CH$_3$−SAM/CH$_3$−SAM system in water.[5,37,38]

Comparing the results presented in Figures 10 and 11, it can be seen that the results obtained from contact angle data confirm the findings from AFM measurement at least qualitatively. The same dependence of adhesion on the hydrophilicity of functional groups of SAMs and quite the same ratios between adhesion values of different groups were found, but the absolute values differ by far. This

(33) Vezenov, D. V.; Noy, A.; Rozsnyai, L. F.; Lieber, C. M. *J. Am. Chem. Soc.* **1997**, *119*, 2006−2015.
(34) Unpublished results of zeta potential measurement, Laboratory of Electrokinetics, Polymer Physics, BASF Aktiengesellschaft.

(35) Israelachvili, J. *Intermolecular and Surface Forces*, 2nd ed.; Academic Press: London, 1992.
(36) Adamson, A. W.; Gast, A. P. *Physical Chemistry of Surfaces*, 6th ed.; Wiley: New York, 1997.
(37) Warszynski, P.; Papastavrou, G.; Wantke, K. D.; Möhwald, H. *Colloids Surf. A* **2003**, *214*, 61−75.
(38) Sinniah, S. K.; Steel, A. B.; Miller, C. J.; Reuth-Robey, J. E. *J. Am. Chem. Soc.* **1996**, *118*, 8925.
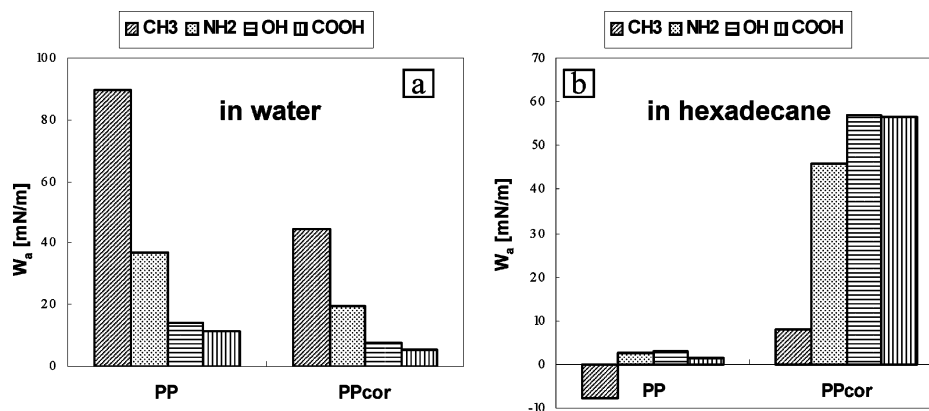
Figure 11. Work of adhesion determined by contact angle analysis (a) for water and (b) for hexadecane as liquid medium.
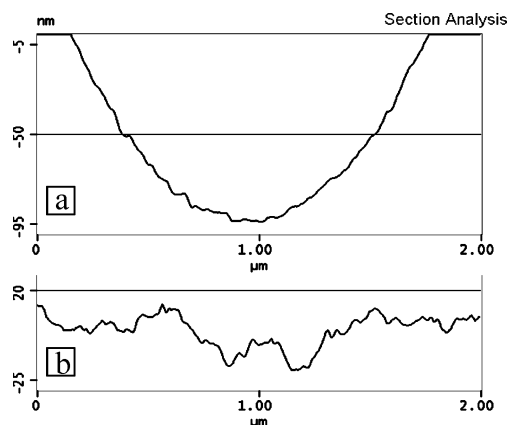

Figure 12. Surface roughness profiles of (a) a gold-coated silica sphere (inverted topography) and (b) corona treated polypropylene film, as determined by AFM.

might be due to the effect of surface roughness that is expected to reduce the work of adhesion as measured by the colloidal probe AFM technique.[39,40]

Effect of Roughness. The roughness of the studied surface influences the force measurements because the contact area is considerably decreased. Figure 12 shows the surface profiles of a gold-coated silica sphere and corona treated polypropylene film obtained by AFM with equal lateral and vertical scale. From comparison of these profiles, it is clear that during a force measurement the sphere can have either a single or several contact points with the sample surface; that is, the contact area is not constant. The force volume mode used here includes 300–500 adhesion force measurements at different spots on the surface, thus averaging over different contact areas. Nevertheless, the comparison of the results obtained by AFM and contact angle measurements (Figures 10 and 11 and Table 5) shows that the work of adhesion is underestimated by the AFM method applied here. This might be due to the roughness effect mentioned above.

For consideration of the effect of roughness on the work of adhesion, the model proposed by Rabinovich et al.[32] was used, which describes the adhesion between nanoscale rough surfaces:

$$F_{\text{pull-off}} = \frac{3\pi W_a R r_2}{2(r_2 + R)} +$$

$$\frac{(AR/6H_0)}{\left(1 + \frac{58R(\text{rms}_1)}{\lambda_1^2}\right)\left(1 + \frac{1.82(\text{rms}_2)}{H_0}\right)^2} \quad (8)$$

where A is the Hamaker constant, R is the radius of the adhering particle, H_0 is the distance of closest approach between surfaces (approximately 0.3 nm), and r_2 is the radius of the asperity, which may be replaced by[32]

$$r_2 = \frac{\lambda_2^2}{58\text{rms}_2} \quad (9)$$

According to Rabinovich, the surfaces exhibit two types of roughness profiles. The first roughness, to be defined as rms_1, is associated with the longer peak-to-peak distance, λ_1 (approximately 800 nm for the polypropylene samples studied in this work). The second, rms_2, occurs on all samples and has a peak-to-peak distance, λ_2, of approximately 180 nm. The peak-to-peak distance was found by analysis of sections taken in different directions from the images. The root-mean-square roughness values estimated by AFM for the surface of untreated PP are $\text{rms}_1 = 9.4$ nm (over an area of $5 \times 5 \ \mu\text{m}^2$) and $\text{rms}_2 = 3.1$ nm (over an area of $0.5 \times 0.5 \ \mu\text{m}^2$), and those for corona treated PP are $\text{rms}_1 = 9$ nm (over an area of $5 \times 5 \ \mu\text{m}^2$) and $\text{rms}_2 = 3$ nm (over an area of $0.5 \times 0.5 \ \mu\text{m}^2$). For a rough estimation of the Hamaker constants between dissimilar materials in nonvacuum media, a modified combining rule approximation[35,41] was used, which gives a relation between the Hamaker constant and surface/interface energies:

$$A_{132} \approx 24\pi D_0^2 \sqrt{|(\gamma_1 + \gamma_3 - 2\gamma_{13})(\gamma_2 + \gamma_3 - 2\gamma_{23})|} \quad (10)$$

The resulting Hamaker constant between untreated PP and CH₃–SAM in water ($A_{132} = 0.41 \times 10^{-20}$ J) agrees well with the values published in the literature[35,42] for alkanes in water ($A_{131} = (0.36–0.49) \times 10^{-20}$ J).

Equation 8 was used for determination of $W_{\text{ad AFM (Rabinovich)}}$ from the experimentally obtained $F_{\text{pull-off}}$. The results are presented in Table 5. The comparison of $W_{\text{ad }\theta}$, $W_{\text{ad AFM (JKR)}}$, and $W_{\text{ad AFM (Rabinovich)}}$ for water as liquid medium shows that the values for the work of adhesion determined by considering the roughness effects are in general much closer to the values from contact angle measurement. However, the values are slightly overestimated for interaction between hydrophobic surfaces in water and underestimated for interaction between hydrophilic surfaces. These discrepancies can be caused by a series of factors. From the point of view of AFM

(39) Götzinger, M.; Peukert, W. *Langmuir* **2004**, *20*, 5298–5303.
(40) Rabinovich, Y. I.; Adler, J. J.; Ata, A.; Singh, R. K.; Moudgil, B. M. *J Colloid Interface Sci.* **2000**, *232*, 17–24.
(41) Gu, Y. *J. Adhesion Sci. Technol.* **2001**, *15*, 1263–1283.
(42) Kokkoli, E.; Zukoshu, C. F. *Langmuir* **2000**, *16*, 6029–6036.

Table 5. Comparison of Work of Adhesion Obtained from Contact Angle Measurements ($W_{ad\ \theta}$) and from AFM Measurements Calculated by Using the JKR ($W_{ad\ AFM\ (JKR)}$) and Rabinovich ($W_{ad\ AFM\ (Rabinovich)}$) Theories

	in water				in hexadecane	
	$W_{ad\ AFM\ (JKR)}$ (mN/m)	$W_{ad\ AFM\ (Rabinovich)}$ (mN/m)	$W_{ad\ \theta}$ (mN/m)	$W_{ad\ \theta}/W_{ad\ AFM\ (Rabinovich)}$	$W_{ad\ AFM\ (JKR)}$ (mN/m)	$W_{ad\ AFM\ (Rabinovich)}$ (mN/m)
PP						
$-CH_3$	14.01 ± 5.20	249.5 ± 92.4	89.7 ± 12.0	0.4	0.02 ± 0.01	0.0 ± 0.1
$-NH_2$	5.91 ± 3.00	105.2 ± 53.4	36.9 ± 11.0	0.4	0.04 ± 0.03	0.3 ± 0.6
$-OH$	0.74 ± 0.55	13.0 ± 9.9	14.3 ± 8.0	1.1	0.04 ± 0.03	0.4 ± 0.5
$-COOH$	1.10 ± 0.62	19.5 ± 11.1	11.2 ± 8.0	0.6	0.05 ± 0.04	0.6 ± 0.6
PPcorona						
$-CH_3$	1.93 ± 1.46	43.7 ± 33.1	44.6 ± 12.0	1.0	0.06 ± 0.04	1.1 ± 0.9
$-NH_2$	0.68 ± 0.37	14.7 ± 8.5	19.5 ± 11.0	1.3	0.18 ± 0.08	3.8 ± 1.9
$-OH$	0.08 ± 0.05	1.1 ± 1.1	7.6 ± 8.0	6.7	0.18 ± 0.07	3.9 ± 1.6
$-COOH$	0.06 ± 0.04	0.5 ± 0.8	5.6 ± 8.0	11.3	0.28 ± 0.14	6.1 ± 3.2

measurement, they are the following: (1) errors in measurement of the radius of the sphere and in estimation of the spring constant of the cantilever, (2) the Rabinovich theory does not take into account the roughness of the colloidal probe, and (3) a hardship with an accurate estimation of the Hamaker constant. From the point of view of contact angle measurement, these factors are the following: (1) error of measurement of contact angle and (2) invalidity of the method for estimation of adhesion work energy from contact angle when spreading takes place. Because of the last reason, a comparison of absolute values of $W_{ad\ \theta}$ and $W_{ad\ AFM}$ for hexadecane as liquid medium makes no sense. The obtained $W_{ad\ AFM\ (Rabinovich)}$ values for hexadecane agree well with values observed in the literature:[3] for the PP/$-OH$ and PPcorona/$-OH$ interactions, which can be seen as chemically identical to $-CH_3/-OH$ and $-OH/-OH$ interactions, respectively, the values of work of adhesion estimated in our study are 0.4 $\pm$ 0.5 and 3.9 $\pm$ 1.6 mN/m and the literature values[3] are 0.6 $\pm$ 0.3 and 4.6. $\pm$ 1.6 mN/m, respectively.

4. Conclusion

The adhesion of various functional groups to polypropylene films was studied using the colloidal probe AFM method in a polar (water) and a nonpolar (hexadecane) liquid medium. A force volume mode was used for the adhesion force measurement. With this averaging procedure, statistically correct values were obtained. The same colloidal probe was coated sequentially with various SAMs. This ensures that differences in the surface roughness of the sphere and uncertainties in spring constant and sphere radius do not directly influence a comparison of the obtained adhesion forces. XPS and contact angle analyses show that the procedure used in this study for the cleaning and recoating of the colloidal probe results in complete removal of an old SAM and in homogeneous deposition of a new one.

The surface physicochemistry of polypropylene films was studied using a number of complementary surface analytical techniques. The surface energy of the films was found to increase, as expected, after corona treatment because of incorporation of oxygen-containing functional groups into the surface of the film.

It was found that the adhesion force has a correlation with the hydrophilic properties of the surfaces of the sample and of the colloidal probe and the polarity of the liquid medium. A maximum adhesive force on corona treated polypropylene film was measured in nonpolar medium with the polar COOH group. A maximum adhesion to untreated PP was found in the polar solvent by interaction with the nonpolar CH_3 group.

From JKR contact mechanics theory, we could directly deduce the experimental work of adhesion between the colloidal probe and the substrate. For verification of the results obtained by AFM, contact angle measurements were carried out and the obtained data were used for a calculation of the thermodynamic work of adhesion. It was shown that the work of adhesion calculated by applying JKR theory was underestimated relative to the values derived from contact angle data because of surface roughness. For a consideration of this effect, the model of Rabinovich was successfully applied. It was shown that colloidal probe AFM in combination with force volume mode is a powerful method for direct measurement of interaction forces not only on model substrates but also on technically relevant systems.